OXFORD

SOT | Society of Toxicology
www.toxsci.oxfordjournals.org

TOXICOLOGICAL SCIENCES, 152(1), 2016, 155–168

doi: 10.1093/toxsci/kfw071
Advance Access Publication Date: April 21, 2016
Research Article

Gene Expression Profiling Identifies Cell Proliferation and Inflammation as the Predominant Pathways Regulated by Aryl Hydrocarbon Receptor in Primary Human Fetal Lung Cells Exposed to Hyperoxia

Binoy Shivanna,*,[1] Suman Maity,† Shaojie Zhang,* Ananddeep Patel,* Weiwu Jiang,* Lihua Wang,* Stephen E. Welty,* John Belmont,‡ Cristian Coarfa,† and Bhagavatula Moorthy*

*Department of Pediatrics, Section of Neonatal-Perinatal Medicine; †Department of Molecular and Cell Biology; and ‡Department of Molecular and Human Genetics, Baylor College of Medicine, Houston, Texas 77030

[1]To whom correspondence should be addressed at Division of Neonatal-Perinatal Medicine, Texas Children's Hospital, Baylor College of Medicine, 1102 Bates Avenue, MC: FC530.01, Houston, Texas 77030. Fax: 832-825-3204. E-mail: shivanna@bcm.edu.

ABSTRACT

Exposure to hyperoxia contributes to the development of bronchopulmonary dysplasia (BPD) in premature infants. We observed that aryl hydrocarbon receptor (AhR) signaling protects newborn mice and primary fetal human pulmonary microvascular endothelial cells (HPMECs) against hyperoxic injury. Additionally, a recent genome-wide transcriptome study in a newborn mouse model of BPD identified AhR as a key regulator of hyperoxia-induced gene dysregulation. Whether the AhR similarly deregulates genes in HPMEC is unknown. Therefore, the objective of this study was to characterize transcriptome level gene expression profile in AhR-sufficient and -deficient HPMEC exposed to normoxic and hyperoxic conditions. Global gene expression profiling was performed using Illumina microarray platform and selected genes were validated by real-time RT-PCR. AhR gene expression and hyperoxia independently affected the expression of 540 and 593 genes, respectively. Two-way ANOVA further identified 85 genes that were affected by an interaction between AhR expression and exposure to hyperoxia. Kyoto Encyclopedia of Genes and Genomes (KEGG), Gene Ontology, and Reactome pathway analysis identified cell proliferation, immune function, cytokine signaling, and organ development as the major pathways affected in AhR-deficient cells. The biological processes that were significantly enriched by hyperoxia included metabolic process, stress response, signal transduction, cell cycle, and immune regulation. Cell cycle was the predominant pathway affected by the combined effect of AhR knockdown and hyperoxia. Functional analysis of cell cycle showed that AhR-deficient cells had decreased proliferation compared with AhR-sufficient cells. These findings suggest that AhR modulates hyperoxic lung injury by regulating the genes that are necessary for cell proliferation and inflammation.

Key words: aryl hydrocarbon receptor; fetal human lung cells; hyperoxia, gene expression profile; organ development.

Bronchopulmonary dysplasia (BPD) is a chronic lung disease of premature infants whose primary structural and functional defect is interrupted alveolarization or alveolar simplification (Husain *et al.*, 1998). BPD is one of the most prevalent complications affecting approximately 14 000 preterm infants born each year in the United States (Fanaroff *et al.*, 2007). Furthermore, infants with BPD are more likely to have long-term pulmonary problems, increased re-hospitalizations during

the first year of life, and neurodevelopmental impairments (Fanaroff *et al.*, 2007; Short *et al.*, 2003). In addition, BPD increases the economic burden with an estimated cost of $2.4 billion per year in United States, making it the second most expensive childhood disease after asthma. Hence, there is an urgent need for improved therapies to prevent and/or treat BPD.

Supplemental oxygen is commonly administered as an important and life-saving measure in patients with impaired lung function. Although oxygen relieves the immediate life-threatening consequences of arterial hypoxemia transiently, it may increase ROS generation and inflammation that can exacerbate lung injury and contribute to the development of BPD (Jobe *et al.*, 2008; Saugstad, 2010; Thiel *et al.*, 2005; Wright and Kirpalani, 2011).

The aryl hydrocarbon receptor (AhR) is a member of basic, helix, loop, helix/PER, ARNT, SIM family of transcriptional regulators (Burbach *et al.*, 1992). AhR activation results in the translocation of the cytosolic AhR to the nucleus, where it regulates the transcription of many phase I and phase II detoxification enzymes such as cytochrome P450 (CYP) 1A1, CYP1A2, glutathione S-transferase-α, NAD(P)H quinone oxidoreductase-1, UDP glucuronosyl transferase, and aldehyde dehydrogenase by binding to the promoter region of the corresponding genes (Emi *et al.*, 1996; Favreau and Pickett, 1991; Rushmore *et al.*, 1990). AhR is required for normal physiological homeostasis (Bock and Kohle, 2009; Fujii-Kuriyama and Kawajiri, 2010; Lindsey and Papoutsakis, 2012; Sauzeau *et al.*, 2011). Additionally, AhR activation has been shown to attenuate tobacco smoke-induced inflammation in the lungs (Baglole *et al.*, 2008; Thatcher *et al.*, 2007), suggesting that AhR is a suppressor of lung inflammation.

The therapies in the early phases of BPD are largely been supportive. Failure to understand the molecular mechanisms that contribute to the development of BPD is one of the main reasons for the lack of specific therapies to prevent and/or treat BPD. Gene expression microarrays allow an unbiased concurrent determination of the transcriptome and are, thus, a powerful tool to identify genes, biological pathways, and their interactions in disease states or experimental exposures, and help investigators understand the molecular mechanisms that contribute to the development of a disease such as BPD. We reported that adult and newborn mice with decreased AhR-signaling are more susceptible to hyperoxic lung injury than wild type mice and this was associated with marked decreases in the expression of detoxifying enzymes (Couroucli *et al.*, 2002; Jiang *et al.*, 2004; Shivanna *et al.*, 2013). Additionally, a recent genome-wide transcriptome study in a newborn mouse model of experimental BPD identified AhR as a key regulator of hyperoxia-induced gene expression responses, many of which are important for cell proliferation, alveolarization, and vascularization (Bhattacharya *et al.*, 2014). Thus, AhR is a potential therapeutic target for BPD. However, to gain mechanistic insights to the development of BPD in humans, it is critical to determine whether AhR contributes to hyperoxia-induced gene dysregulation in primary neonatal human lung cells. The fetal human pulmonary microvascular endothelial cells (HPMECs) express AhR (Kato *et al.*, 1997) and are used to examine mechanisms of hyperoxic injury in human fetal lung cells (Wright *et al.*, 2010). Furthermore, we used these cells to demonstrate that AhR is necessary to attenuate hyperoxic injury (Zhang *et al.*, 2015). Hence, we performed microarray experiments to characterize transcriptome level gene expression patterns in AhR-sufficient and -deficient HPMEC in an effort to determine the molecular mechanisms by which AhR modulates hyperoxic injury in primary fetal human lung cells.

MATERIALS AND METHODS

Cell Culture

HPMEC, the primary microvascular endothelial cells derived from human fetal lungs were obtained from ScienCell research laboratories (San Diego, California; 3000). HPMEC were grown in 95% air and 5% CO_2 at 37°C in specific endothelial cell medium according to the manufacturer's protocol.

Small Interfering RNA Transfections

HPMEC were seeded in fibronectin-coated 6-well plates at 60–70% confluence 24 h before transfection. Transfections were then performed with either 50 nM control small interfering RNA (siRNA) (Dharmacon, Lafayette, Colorado; d-001810) or 50 nM AhR specific siRNA (Dharmacon, Lafayette, Colorado; L-004990) using LipofectamineRNAiMAX (Life Technologies, Grand Island, New York; 13778030). Twenty-four hours after transfections, the cells were exposed to air or hyperoxia for up to 24 h. siRNA mediated knockdown of AhR was validated by determining the expression of AhR mRNA and protein by real time RT-PCR analysis and western blotting, respectively. Additionally, cells were harvested and analyzed for gene expression profile and cell proliferation.

Exposure of Cells to Hyperoxia

Hyperoxia experiments were conducted in a plexiglass sealed chamber placed in a Forma Scientific water-jacketed incubator at 37°C. A mixture of 95% O_2 and 5% CO_2 gas was circulated continuously into the sealed chamber and the oxygen concentration inside the chamber was checked intermittently with an oxygen analyzer. Once the O_2 level inside the chamber reached 95%, the cells were placed inside the chamber for the desired length of time (Shivanna *et al.*, 2011). Since our previous study using this model had demonstrated that AhR is necessary to protect HPMEC against hyperoxic injury (Zhang *et al.*, 2015), we used the same model to further our understanding of how AhR modulates hyperoxic injury in this model.

RNA Isolation and Purification

HPMEC grown in 6 well plates were transfected with control or AhR siRNA as described earlier for 24 h, following which they were exposed to air or hyperoxia. At 24 h of exposure, total RNA was isolated and purified with an on-column DNAse I treatment by using the Direct-zol RNA MiniPrep kit (Zymo Research, Irvine, California; R2052) according to the manufacturer's protocol. The quality of the RNA was assessed using spectrophotometry (NanoDrop-1000 Spectrophotometer, Thermo Fisher Scientific) and microfluidic electrophoresis (Experion Automated Electrophoresis System, Bio-Rad Laboratories). RNA samples with a concentration >50 ng/μl and an integrity number >6, a numerical scale measure of intact RNA, were used for microarray analysis. Our rationale for determining the gene expression profile at 24 h of exposure to normoxia (air) or hyperoxia was to increase the likelihood of identifying differential gene expression and their associated biological processes. This time point was based on the differential gene expression that was seen between hyperoxia-exposed AhR-sufficient and -deficient cells at 24 h in our previous study (Zhang *et al.*, 2015).

Microarray Analysis

Ambion Illumina TotalPrep RNA Amplification Kit (Applied Biosystems/Ambion) was used to synthesize cRNA as per the manufacturer's recommendations. The cRNA samples were subjected to quality control using spectrophotometry (NanoDrop-1000 Spectrophotometer, Thermo Fisher Scientific) and microfluidic electrophoresis (Experion Automated Electrophoresis System, Bio-Rad Laboratories), before they were hybridized onto Illumina Human HT-12v3 Expression BeadChips (Illumina, San Diego, California) according to the manufacturer's protocol. The BeadStudio analysis software was used to apply the standard quality control thresholds, and failed microarrays were removed (Du *et al.*, 2008).

Microarray Data Processing

Lumi package in R statistical software, version 2.14.1 (Du *et al.*, 2008), was used to perform quality control of the signal intensity data on the transcript probes, background adjustment, variance stabilization transformation, and rank invariant normalization. A detection *P*-value cutoff of 0.01 was required for the normalized intensities to consider a transcript as detected.

Differential Gene Expression Analyses

Differential gene expression analyses of AhR-sufficient and -deficient cells exposed to air or hyperoxia were performed using *limma* R package (Wettenhall and Smyth, 2004). The effects of AhR, exposure, and their associated interactions for the differentially expressed genes (DEGs) were assessed using the ANOVA methodology, with correction for multiple comparisons performed using the Benjamini Hochberg adjustment method; we employed these methods as implemented in the R statistical system. Statistical significance of genes for individual variables (AhR, exposure) was considered for false discovery rate (FDR)-adjusted $q < 0.05$ and the fold change exceeding 1.5×. Genes were considered significant for interaction by ANOVA method if FDR-adjusted $q < 0.2$. The heatmap of mean-centered normalized expression values and unsupervised hierarchical clustering of the samples based on euclidean distances of expression profiles to assess grouping was performed using the heatmap function in R statistical software.

Pathway Enrichment and Content Analysis

The DEG were subjected to pathway enrichment and content analysis using the gene set collections KEGG (Kanehisa *et al.*, 2014), REACTOME (Croft *et al.*, 2014), and Gene Ontology (Ashburner *et al.*, 2000) Biological Processes as collated by the Molecular Signature Databases (MSigDB, http://www.broadinstitute.org/gsea/msigdb) compendium (Subramanian *et al.*, 2005). A gene set was considered significantly enriched for $p < .05$ (hypergeometric distribution).

Quantitative real-Time RT- PCR Assays

HPMEC grown in 6-well plates were transfected with control or AhR siRNA as described earlier for 24 h, following which they were exposed to air or hyperoxia. At 24 h of exposure, the total RNA extracted from the cells using Direct-zol RNA MiniPrep kit (Zymo Research, Irvine, California; R2052) and reverse transcribed to cDNA as described earlier (Zhang *et al.*, 2015). Real-time quantitative RT-PCR analysis was performed with 7900HT Real-Time PCR System using TaqMan gene expression master mix (Grand Island, New York; 4369016) and gene specific primers (Grand Island, NY; AhR-Hs00169233_m1; BCAT1-Hs00398962_m1; CCL5-Hs00982282_m1; CDC20-Hs00426680_mH; CXCL10-Hs01124252_g1; CYP1A1-Hs01054797_g1; GAPDH-Hs02758991_g1; Karyopherin alpha 2 (KPNA2)-Hs00818252_g1; PGF-Hs00182176_m1). These genes were selected based upon their robust differential expression on microarray analysis and their relevance to oxygen toxicity. GAPDH was used as the reference gene. The samples were denatured at 95 °C for 10 min followed by a thermal cycling step of 40 cycles at 95 °C for 15s and 40 cycles at 60 °C for 1 min. The $\Delta\Delta C_t$ method was used to calculate the fold change in mRNA expression.

Cell Proliferation Assay

Cell proliferation was determined based on the measurement of cellular DNA content via fluorescent dye binding using the CyQUANT NF cell proliferation assay kit (Invitrogen, Carlsbad, Californnia; C35006) as per the manufacturer's recommendations. HPMEC seeded onto 96-well microplates were grown to 60–70% confluence, before being transfected with 50 nM control or AhR siRNA. After 24 h of transfection, the cells were exposed to air or hyperoxia for 48 h. At the end of experiments, the medium was gently aspirated, and the cells were incubated for 30 min with 100 µl of 1× dye-binding solution per well. Following the incubation, the fluorescence intensity of each sample was measured using Spectramax M3 fluorescence microplate reader with excitation at 485 nm and emission detection at 530 nm.

Analyses of Real Time RT-PCR and Cell Proliferation Data

The results were analyzed by GraphPad Prism 5 software. At least 3 separate experiments were performed for each measurement, and the data are expressed as means ± SEM. The effects of AhR gene expression, gas exposure, and their associated interactions for the outcome variables were assessed using ANOVA techniques. Multiple comparison testing by the posthoc Bonferroni test was performed if statistical significance of either variable or interaction was noted by ANOVA. A *P*–value of <.05 was considered significant.

RESULTS

Validation of AhR Knockdown in HPMEC

To characterize the differential gene expression between AhR-sufficient and -deficient HPMEC, we initially performed AhR siRNA transfection experiments to knockdown AhR in HPMEC. AhR siRNA significantly decreased the expression of both AhR mRNA (Figure 1A) and protein (Figure 1B) in normoxic (air) and hyperoxic conditions.

Analysis of DEGs

To identify the AhR-dependent gene expression in hyperoxic conditions, genome-wide microarray expression studies were conducted in AhR-sufficient and -deficient cells exposed to air or hyperoxia. None of our biological samples failed quality control. Our principle component analysis (Figure 2) revealed that the samples to be clustered according to the AhR gene expression and oxygen exposure, which suggests that the differential expression is unlikely due to the technical variation between the biological replicates. The dataset will be deposited in NCBI's Gene Expression OMNIBUS (GEO).

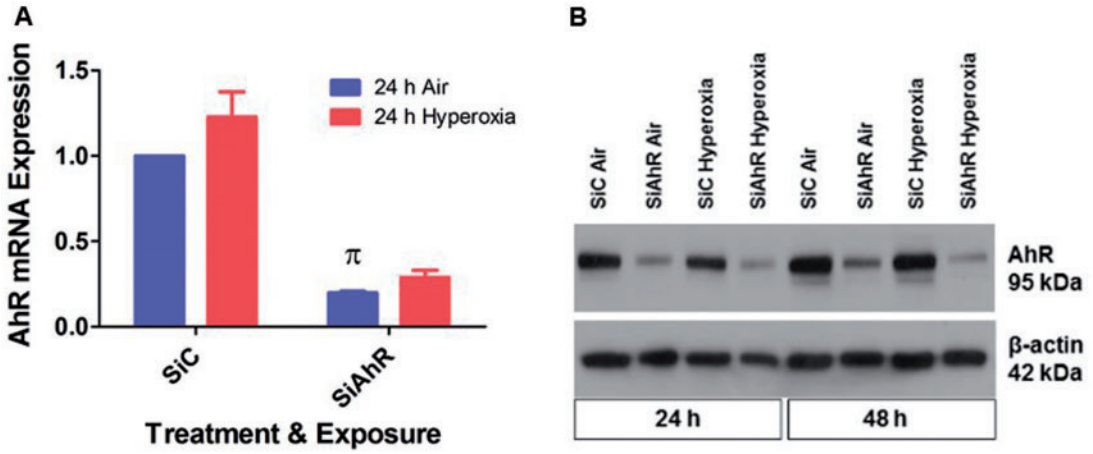

FIG. 1. Validation of siRNA mediated knockdown of AhR in HPMEC. HPMEC were transfected with either 50 nM control (SiC) or AhR (SiAhR) siRNA and exposed to air or hyperoxia for up to 48 h, following which RNA was extracted for real-time RT-PCR analyses of AhR mRNA **(A)** expression. In addition, whole-cell protein was extracted for western blot analysis with the anti-AhR or anti-β-actin antibodies **(B)**. Data are representative of at least 3 independent experiments. Values are presented as means ± SEM (n = 3). π, $P < .05$ versus control siRNA.

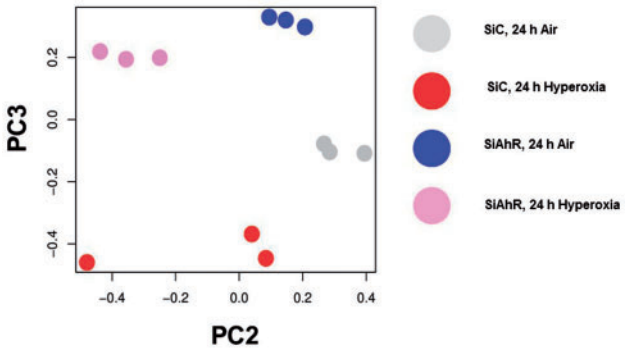

FIG. 2. Principal component analysis (PCA) of the microarray experiments. The PCA of control (SiC) and AhR (SiAhR) transfected HPMEC exposed to air or hyperoxia for 24 h shows clustering of genes profiles in respective groups.

Analysis of DEGs and Pathways Based on AhR Gene Expression

Analysis of DEG between AhR-sufficient and -deficient cells showed 540 genes to be significantly regulated by AhR at FDR-adjusted $q < 0.05$ and fold change exceeding 1.5× (see Supplementary Table 1 for the entire list). Heatmap of the mean-centered, normalized expression levels of the DEG based on the AhR gene expression (FDR-corrected P-value $< .05$, FC ≥ 1.5) demonstrate that the gene expression profiles of AhR-sufficient cells can be distinguished from those of AhR-deficient cells (Figure 3A). AhR deficiency resulted in significant differential expression of genes (n = 294) in hyperoxia compared with normoxia (Figs. 3B and C). In AhR-deficient cells, 239 genes were down-regulated (Figure 3B) and 301 genes were up-regulated (Figure 3C) when compared with AhR-sufficient cells. Among the down-regulated genes in the AhR-deficient cells, 146 and 27 genes were exclusively down-regulated in hyperoxic and air conditions, respectively, with 66 genes being mutually down-regulated by both conditions (Figure 3B). Of the up-regulated genes in AhR-deficient cells, 148 and 49 genes were exclusively up-regulated in hyperoxic and air conditions, respectively, with 104 genes being mutually up-regulated by both conditions (Figure 3C).

We next determined how the DEGs affect the biological process in AhR-deficient cells compared with AhR-sufficient cells in air and hyperoxic conditions by performing pathway analysis using KEGG, Reactome and Gene Ontology databases. These DEGs highly enriched functions related to immune regulation, metabolic process, cell cycle, and signal transduction (Figure 4). Up-regulated genes (Tables 2 and 4) were enriched for molecular processes such as antigen processing, interferon signaling, cytokine receptor interactions, and pyrimidine catabolism indicating the activation of these pathways in AhR-deficient cells (Figure 4B). In contrast, the down-regulated genes (Tables 1 and 3) were significantly enriched for biological processes specific to organ development, integrin cell surface interactions, cell adhesion, cell proliferation, and cancer development indicating repression of these pathways in AhR-deficient cells (Figure 4A). The complete list of deregulated biological process based on AhR gene expression is shown in Supplemental Table 2.

Analysis of DEGs and Pathways Based on Exposure to Hyperoxia

Analysis of differential gene expression between air and hyperoxia exposed cells showed 593 genes to be significantly regulated by hyperoxia at $P < .05$ (adjusted P-value; see Supplemental Table 3 for the entire list). Heatmap of the mean-centered, normalized expression levels of the DEGs based on exposure (FDR-corrected q-value < 0.05, FC ≥ 1.5) demonstrate that the gene expression profiles of hyperoxia-exposed cells can be distinguished from those of air-exposed cells (Figure 5A). In hyperoxia-exposed cells, 304 genes were down-regulated (Figure 5B), and 289 genes were up-regulated (Figure 5C) when compared with air-exposed cells. Among the down-regulated genes in hyperoxia-exposed cells, 76 and 136 genes were exclusively down-regulated in AhR-deficient and -sufficient cells, respectively, with 92 genes being mutually down-regulated in both cell phenotypes when compared with corresponding air-exposed cells (Figure 5B). Of these up-regulated genes, 104 and 84 genes were exclusively up-regulated in AhR-deficient and-sufficient cells, respectively, with 101 genes being mutually up-regulated in both cell phenotypes when compared with corresponding air-exposed cells (Figure 5C). There were significantly more genes up-regulated than down-regulated in AhR-deficient than -sufficient cells upon exposure to hyperoxia (Figs. 5B and C).

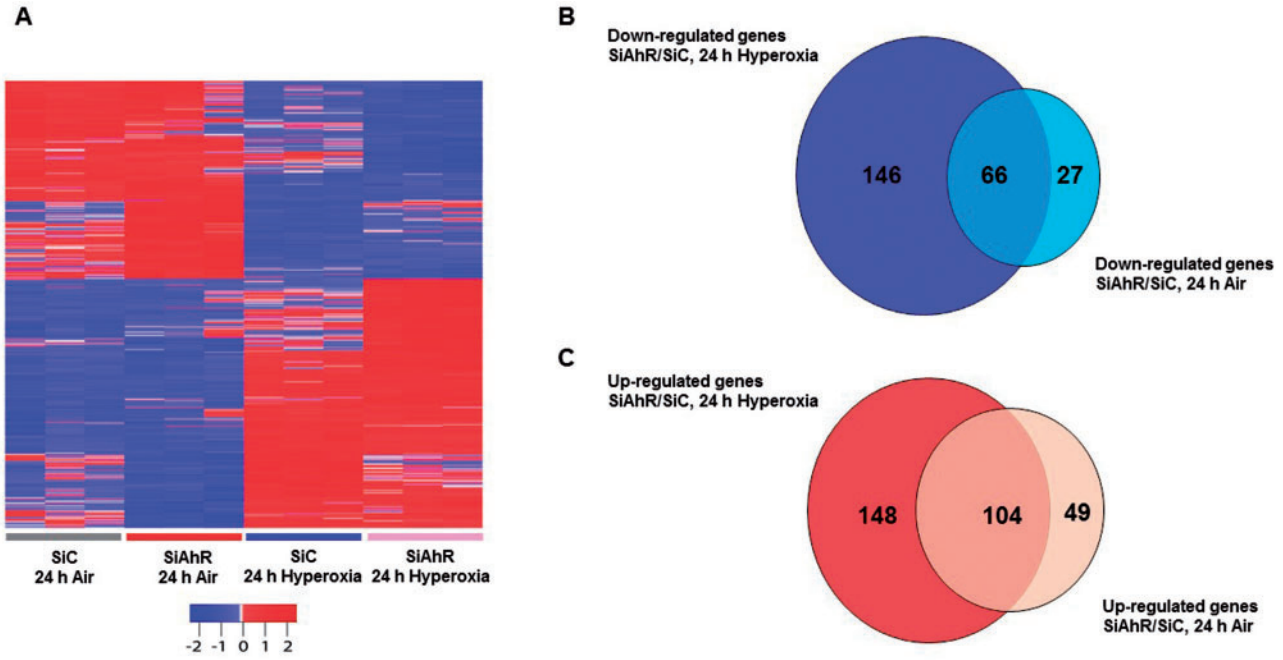

FIG. 3. Microarray analysis of AhR-modulated genes. **A,** Heatmap analysis of probes with >1.5-fold change in their expression. Data represent fold change for each condition compared with that for AhR-sufficient cells. Venn diagrams showing the down-regulated **(B)** and up-regulated **(C)** genes in AhR siRNA transfected cells (SiAhR) exposed to hyperoxic and normoxic (air) conditions compared with similarly exposed control siRNA-transfected cells (SiC).

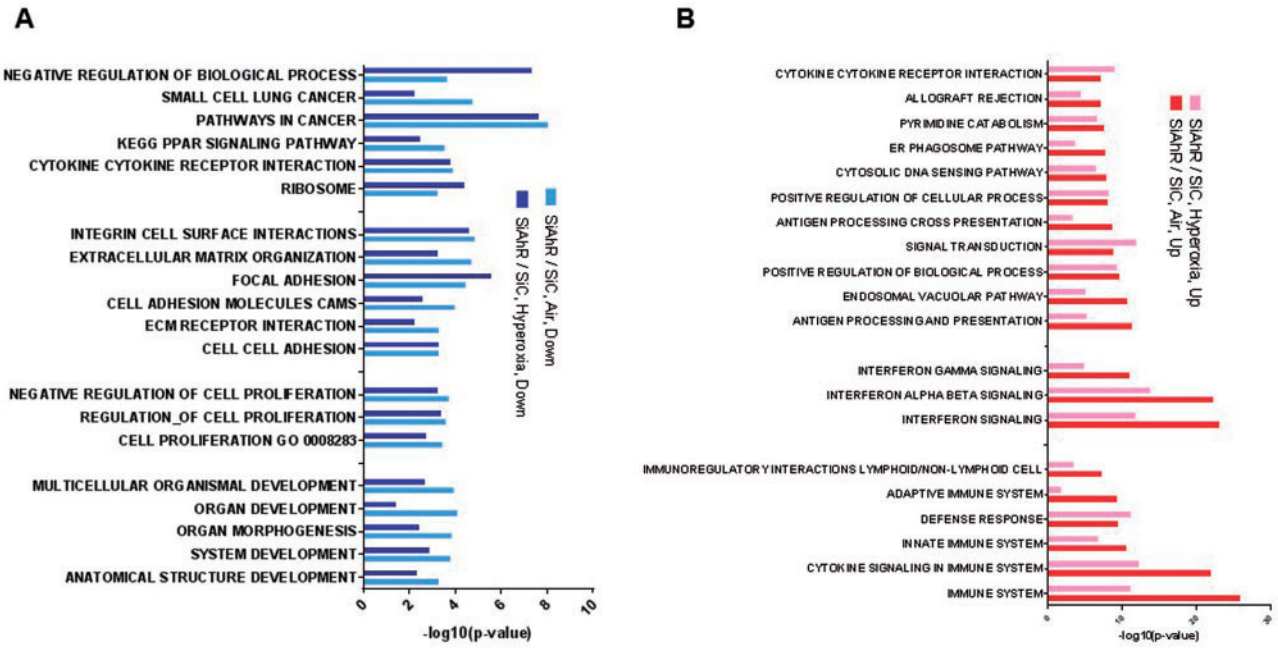

FIG. 4. Microarray analysis of AhR-modulated pathways. **A,** Top down-regulated and **B,** Top up-regulated pathways affected by the AhR gene expression.

The biological processes that were significantly enriched by hyperoxia included metabolic process, response to stress, signal transduction, cell cycle, and immune regulation (Figure 6). Up-regulated genes (Tables 6 and 8) were enriched for molecular processes specific to inflammation, cytokine receptor interaction, stress response, cell death, and metabolism indicating the activation of these pathways in hyperoxia-exposed cells (Figure 6B). In contrast, the downregulated genes (Tables 5 and 7) were significantly enriched for biological processes specific to cell cycle indicating repression of this pathway in hyperoxia-exposed cells (Figure 6A). The complete list of deregulated biological process based on exposure status is shown in Supplemental Table 4.

Analysis of DEGs and Pathways Based on Interaction between AhR Gene Expression and Exposure to Hyperoxia

Two-way ANOVA showed that AhR gene interacts with hyperoxia to differentially regulate 85 genes (FDR-adjusted q-value < 0.2; see Supplemental Table 5 for the entire list). Heatmap of the mean-

TABLE 1. Top 10 Down-Regulated Genes by the AhR in Air-Exposed HPMEC

Gene Name	Gene Symbol	BH.P-Value	Fold Change SiAhR versus SiC
ACVRL1	ACVRL1	0.004411	0.662842
Chemokine (C-C motif) Ligand 2	CCL2	0.003251	0.57346
Cyclin D2	CCND2	0.001217	0.63687
Collagen Type IV Alpha 2	COL4A2	0.010867	0.602644
Avian erythroblastosis virus E26 (v-ets) oncogene homolog-1	ETS1	0.041854	0.626621
Lymphotoxin-beta	LTB	0.004199	0.4641
Coagulation factor II (thrombin) receptor-like 1	F2RL1	0.02946	0.583065
Laminin gamma 2	LAMC2	0.003247	0.599715
Branched chain amino-acid transaminase 1	BCAT1	0.024418	0.608396
Collagen Type IV Alpha 1	COL4A1	0.018601	0.656937

TABLE 2. Top 10 Up-Regulated Genes by the AhR in Air-Exposed HPMEC

Gene Name	Gene Symbol	BH.P-Value	Fold Change SiAhR versus SiC
Proteasome subunit beta type-8	PSMB8	0.011596	1.528944
Chemokine (C-C motif) Ligand 5	CCL5	0.005603	2.7937
Proteasome subunit beta type-9	PSMB9	0.039947	1.919102
Chemokine (C-X-C motif) ligand 10	CXCL10	0.003695	2.149835
Cluster of differentiation 74	CD74	0.003595	1.57702
Interferon beta 1	IFNB1	0.001571	1.843581
Toll-like receptor 3	TLR3	0.00238	1.633283
Angiopoietin-like 4	ANGPTL4	0.000874	1.862461
Human leukocyte antigen G	HLA-G	0.011271	1.960357
Tumor necrosis factor (ligand) superfamily, member 10	TNFSF10	0.00584	2.173982

TABLE 3. Top 10 Down-Regulated Genes by the AhR in Hyperoxia-Exposed HPMEC

Gene Name	Gene Symbol	BH.P-Value	Fold Change SiAhR versus SiC
Small mothers against decapentaplegic homolog 3	SMAD3	0.013429	0.559079
Cyclin-dependent kinase inhibitor 1A	CDKN1A	0.025845	0.665021
Tumor necrosis factor	TNF	0.009499	0.577694
ACVRL1	ACVRL1	0.004411	0.577028
Chemokine (C-C motif) ligand 2	CCL2	0.003251	0.617562
BCL2-associated agonist of cell death	BAD	0.01694	0.662784
Calmodulin 1	CALM1	0.006597	0.666117
Cyclin D2	CCND2	0.000146	0.619838
Kruppel-like factor 11	KLF11	0.005045	0.63133
MAX dimerization protein 4	MXD4	0.000319	0.531299

Table 4. Top 10 Up-Regulated Genes by the AhR in Hyperoxia-Exposed HPMEC

Gene Name	Gene Symbol	BH.P-Value	Fold Change SiAhR versus SiC
Chemokine (C-C motif) Ligand 5	CCL5	0.005603	2.144558
Chemokine (C-C motif) ligand 3	CCL3	0.024253	1.522869
Zinc finger and BTB domain containing 16	ZBTB16	0.000479	1.569467
Kruppel-like factor 4	KLF4	0.048839	1.71244
Chemokine (C-X-C motif) ligand 10	CXCL10	0.003695	2.100208
Adrenoceptor Beta 2	ADRB2	0.001428	1.586095
Follistatin	FST	0.001188	2.393585
Annexin A1	ANXA1	0.021502	1.520234
KPNA2	KPNA2	0.011625	1.601478
Primase, DNA, polypeptide 1	PRIM1	0.030688	1.957271

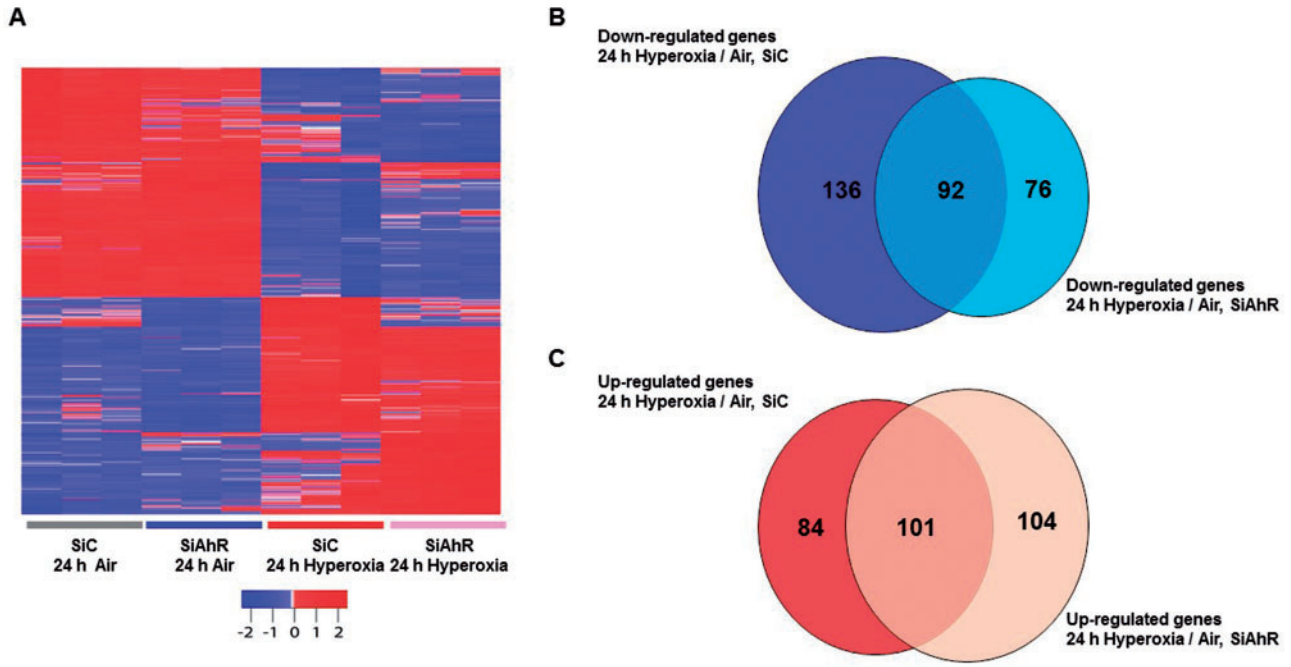

FIG. 5. Microarray analysis of hyperoxia-regulated genes. **A,** Heatmap analysis of probes with >1.5-fold change in their expression. Data represent fold change for each condition compared with that for hyperoxia-exposed cells. Venn diagrams showing the down-regulated **(B)** and up-regulated **(C)** genes in AhR-sufficient (SiC) and -deficient (SiAhR) cells in hyperoxic conditions compared with normoxic (air) conditions.

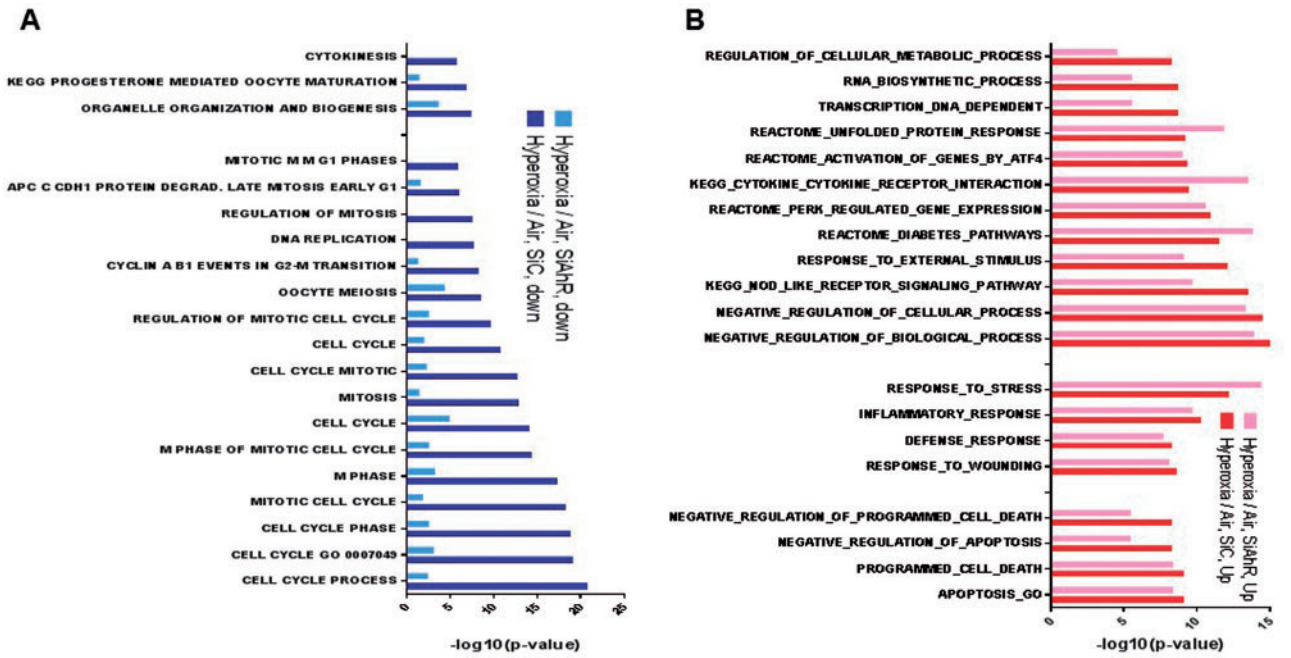

FIG. 6. Microarray analysis of hyperoxia-modulated pathways. **A,** Top down-regulated and **B,** Top up-regulated pathways affected by the exposure of cells to hyperoxia.

centered, normalized expression levels of the DEGs based on the interaction between AhR gene expression and exposure to hyperoxia demonstrate that the gene expression profiles of AhR-sufficient cells can be distinguished from those of AhR-deficient cells both in air and hyperoxic conditions (Figure 7A).

The top 10 DEGs based on the interaction between AhR gene expression and exposure to hyperoxia are shown in Table 9. The major deregulated pathways based on the interaction between AhR gene and hyperoxia were related to cell cycle, catalytic activity, and metabolism (Figure 7B).

Quantitative real-Time RT-PCR Validation of Microarray Result in AhR-Sufficient and -Deficient HPMEC

Based on their relevance to oxygen toxicity, we selected 6 (BCAT1, CCL5, CDC20, CXCL10, KPNA2, and placental growth

TABLE 5. Top 10 Down-Regulated Genes by Hyperoxia in Control siRNA (SiC)-Transfected HPMEC

Gene Name	Gene Symbol	BH.*P*-Value	Fold Change Hyperoxia versus Air
Ubiquitin-conjugating enzyme E2C	UBE2C	0.00059	0.513744
Baculoviral IAP repeat containing 5	BIRC5	0.001563	0.522019
CDC20	CDC20	0.00456	0.272116
KPNA2	KPNA2	0.001557	0.545562
Heat Shock Protein 90 kDa Alpha, Class A Member 1	HSP90AA1	0.012027	0.595519
Cyclin A2	CCNA2	0.002769	0.468611
Cyclin A1	CCNA1	0.003886	0.364467
24-dehydrocholesterol reductase	DHCR24	0.004742	0.469648
S-phase kinase-associated protein 2	SKP2	0.010684	0.588967
Polo-like kinase 1	PLK1	0.001758	0.62096

TABLE 6. Top 10 Up-Regulated Genes by Hyperoxia in Control siRNA (SiC)-Transfected HPMEC

Gene Name	Gene Symbol	BH.*P*-Value	Fold Change Hyperoxia versus Air
Tumor necrosis factor	TNF	0.00409	1.881026
Interleukin 6	IL6	0.00407	1.958738
Interleukin 8	IL8	0.001002	1.765375
Chemokine (C-C motif) ligand 2	CCL2	0.002891	1.648113
Activating transcription factor 4	ATF4	0.014547	1.589246
Chemokine (C-C motif) ligand 5	CCL5	0.003886	3.015285
ATP-binding cassette subfamily A member 1	ABCA1	0.003273	1.532424
Cbp/P300-interacting transactivator, with Glu/Asp-rich carboxy-terminal domain, 2	CITED2	0.007346	1.595904
Kruppel-like factor 4	KLF4	0.007443	1.81925
Nuclear receptor-interacting protein 1	NRIP1	0.034146	1.616488

TABLE 7. Top 10 Down-Regulated Genes by Hyperoxia in AhR siRNA (SiAhR)-Transfected HPMEC

Gene Name	Gene Symbol	BH.*P*-Value	Fold Change Hyperoxia versuus Air
ACVRL1	ACVRL1	0.005685	0.59763
Aurora kinase A	AURKA	0.00257	0.633603
CDC20	CDC20	0.00456	0.519025
Histone deacetylase 1	HDAC1	0.004387	0.583837
Heat shock 70 kDa protein 1B	HSPA1B	0.003443	0.585998
HIV-1 Tat interactive protein 2	HTATIP2	0.010355	0.631972
Integrin, Beta 1	ITGB1	0.036699	0.53885
K(Lysine) acetyltransferase 2A	KAT2A	0.011237	0.56817
Mitogen-activated protein kinase 1	MAPK1	0.000878	0.663609
Ras-related C3 botulinum toxin substrate 2	RAC2	0.005628	0.577899

TABLE 8. Top 10 Up-Regulated Genes by Hyperoxia in AhR siRNA (SiAhR)-Transfected HPMEC

Gene Name	Gene Symbol	BH.*P*-value	Fold Change Hyperoxia versus Air
Chemokine (C-C motif) ligand 2	CCL2	0.002891	1.774859
Interleukin 6	IL6	0.00407	3.221077
Interleukin 8	IL8	0.001002	2.13187
Chemokine (C-C motif) ligand 5	CCL5	0.003886	2.314655
Chemokine (C-C motif) ligand 3	CCL3	0.017009	1.545059
ATP-binding cassette subfamily A member 1	ABCA1	0.003273	1.535272
Kruppel-like factor 4	KLF4	0.017751	1.878612
Interleukin 1A	IL1A	0.00409	2.650247
Follistatin	FST	0.005962	1.806616
Interferon beta 1	IFNB1	0.01146	2.363033

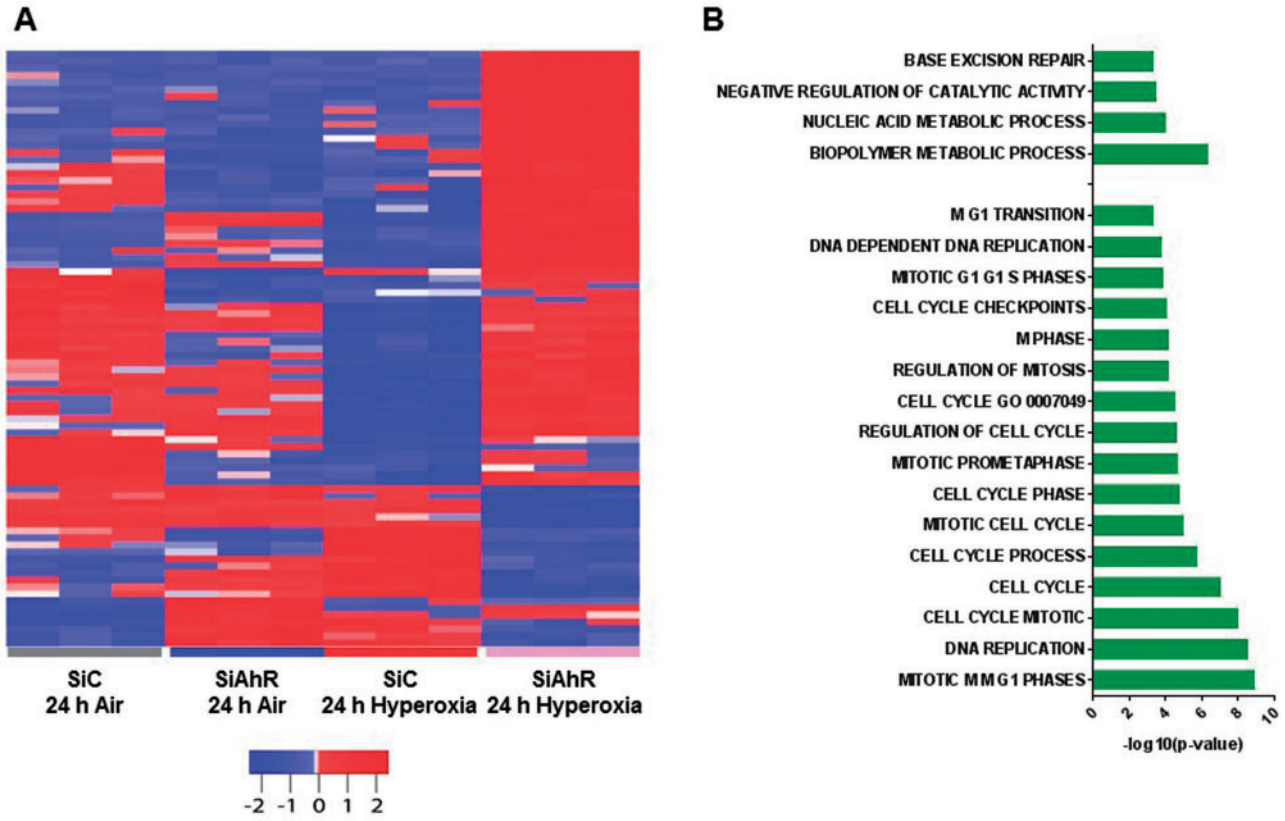

FIG. 7. Microarray analysis of DEGs based on interaction of AhR with hyperoxia. **A,** Heatmap analysis of probes with >1.5-fold change in their expression. Data represent fold change for each condition as a result of interaction of the AhR gene with hyperoxia. **B,** Top pathways affected by interaction of the AhR gene with hyperoxia.

TABLE 9. Top 10 De-Regulated Genes by an Interaction Between AhR and Hyperoxia

Gene Name	Gene Symbol	BH.P-Value
KPNA2	KPNA2	0.136
Ubiquitin-conjugating enzyme E2C	UBE2C	0.196
Polymerase (RNA) II (DNA directed) polypeptide K	POLR2K	0.196
Nucleolar- and spindle-associated protein 1	NUSAP1	0.196
Chemokine (C-C motif) ligand 3	CCL3	0.199
MAD2 mitotic arrest deficient-like 1	MAD2L1	0.199
Nucleolar protein 58	NOP58	0.184
Timeless interacting protein	TIPIN	0.184
Chemokine (C-C Motif) receptor 2	CCR2	0.196
High mobility group box 2	HMGB2	0.196

factor [PGF]) differentially regulated genes on the microarrays for validation by real-time RT-PCR. The microarray data was confirmed in 5 of the 6 (83%) genes tested (Figs. 8 and 9). BCAT gene was not deregulated by the AhR gene or exposure in our validation experiments (Figure 8C). In general, the magnitude change in gene expression identified by the microarray experiments correlated with that of real-time RT-PCR data except for the chemokines, CCL5, and CXCL10. In hyperoxic conditions, the fold changes measured by real-time RT-PCR (Figure 9) were 12–24 times greater than those seen in the array data for the chemokines, CCL5 (array: 2-fold increase; real time RT-PCR: 24-fold increase) and CXCL10 (array: 2-fold increase; real time RT-PCR: 45-fold increase), respectively. To our surprise, the AhR-regulated prototypical target gene, CYP1A1, was not deregulated in microarray analysis. Hence, we determined CYP1A1 mRNA expression in our experimental conditions. Consistent with our previous data, CYP1A1 mRNA expression was decreased in AhR-deficient cells by 87 and 93%in air and hyperoxic conditions, respectively (Figure 10).

Cell Proliferation Analysis of AhR-Sufficient and -Deficient HPMEC

The identification of cell cycle as the major biological pathway affected by the DEG in our experimental model prompted us to finally investigate the effects of AhR on cell proliferation. The mean fluorescence of AhR-sufficient and -deficient cells in air conditions were 3193.37 and 3080.83, respectively. Upon hyperoxia exposure, the mean fluorescence of these cells decreased to 2753.83 and 2320.43, respectively (Figure 11). Two-way ANOVA of CyQUANT NF cell proliferation assay showed that AhR interacts with hyperoxia to decrease cell proliferation (Figure 11), which suggests that AhR is necessary for cell cycle progression in hyperoxic conditions.

DISCUSSION

Animal studies have clearly demonstrated that pulmonary vascular and alveolar development are interdependent processes and an interruption of distal lung angiogenesis leads to alveolar simplification (vascular hypothesis) (Abman, 2001). This study applies bioinformatics to understand the molecular mechanisms by which AhR modulates oxygen toxicity in primary fetal HPMEC and thereby provides a rationale for future *in vitro* and

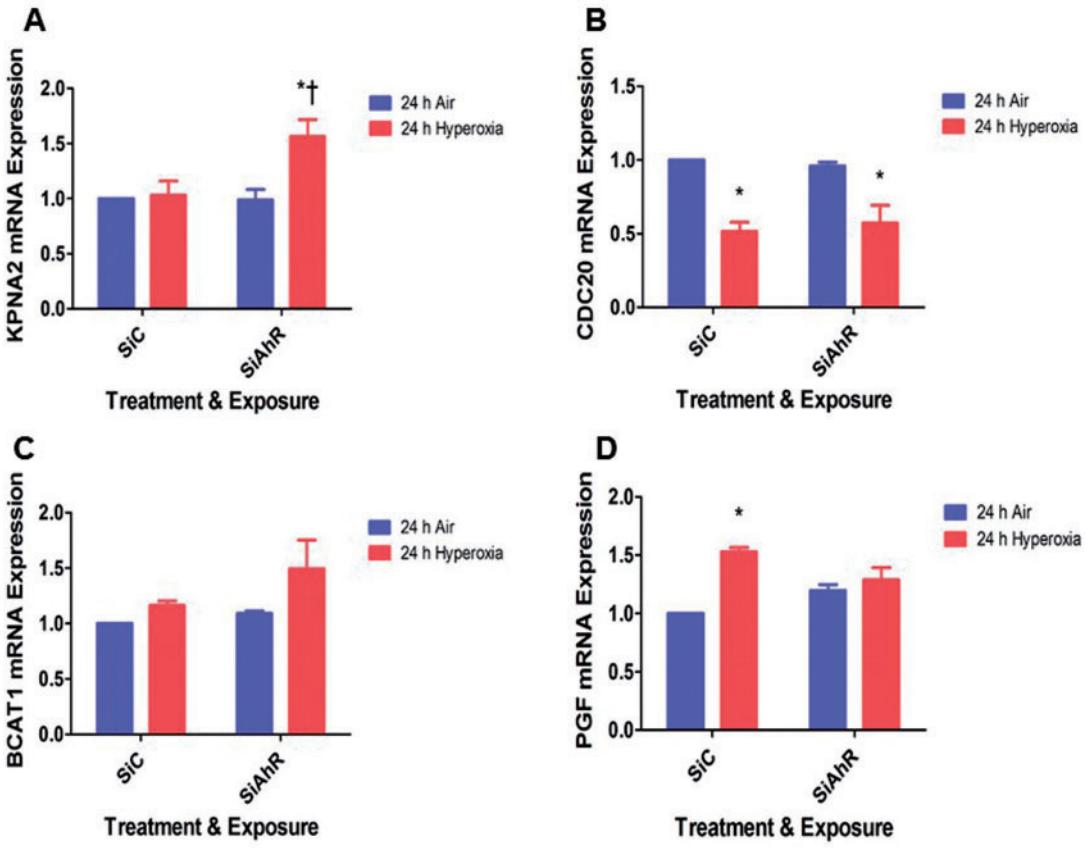

FIG. 8. Real-time RT-PCR validation of genes affecting the cell proliferation. Control (SiC) or AhR (SiAhR) siRNA-transfected HPMEC were exposed to normoxia (air) or hyperoxia for up to 24 h, following which RNA was extracted for real-time RT-PCR analyses of KPNA2 **(A)**, CDC20 **(B)**, BCAT1 **(C)**, and PGF **(D)** mRNA expression. Data are representative of at least 3 independent experiments. Values are presented as means ± SEM (n = 3). Two-way ANOVA showed an effect of hyperoxia for the dependent variables, KPNA2, PGF2, and CDC20, and of AhR gene for the dependent variable, KPNA2. An interaction effect was seen for the dependent variables, KPNA2 and PGF2, in this figure. Significant differences between air- and hyperoxia-exposed cells are indicated by *, $P < .05$. Significant differences between hyperoxia-exposed AhR-sufficient and -deficient cells are indicated by †, $P < .05$.

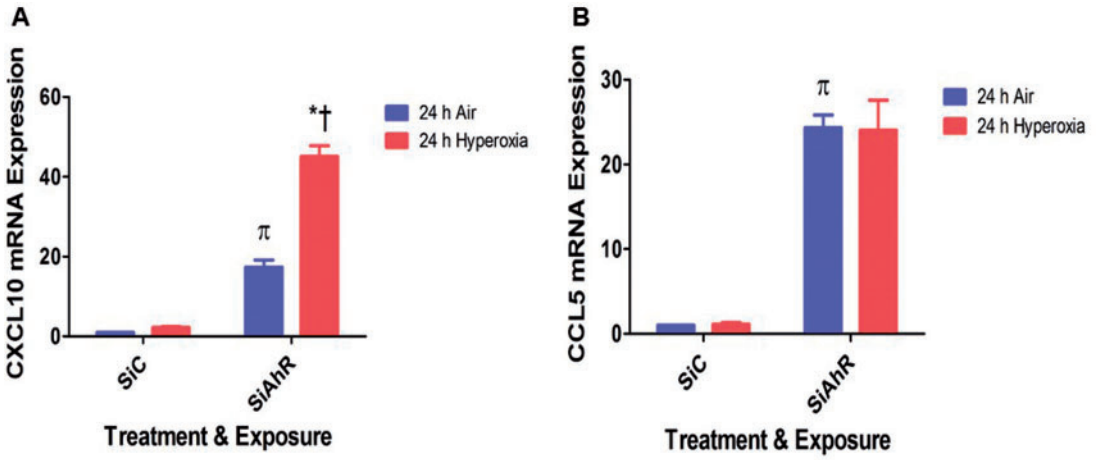

FIG. 9. Real-time RT-PCR validation of genes affecting the inflammatory response. Control (SiC) or AhR (SiAhR) siRNA-transfected HPMEC were exposed to normoxia (air) or hyperoxia for up to 24 h, following which RNA was extracted for real-time RT-PCR analyses of CXCL10 **(A)** and CCL5 **(B)** mRNA expression. Data are representative of at least 3 independent experiments. Values are presented as means ± SEM (n = 3). Two-way ANOVA showed an effect of hyperoxia and AhR gene and an interaction between them for the dependent variable, CXCL10, in this figure. Significant differences between air- and hyperoxia-exposed cells are indicated by *, $P < .05$. Significant differences between hyperoxia-exposed AhR-sufficient and –deficient cells are indicated by †, $P < .05$. Significant differences between air-exposed cells are indicated by π, $P < .05$.

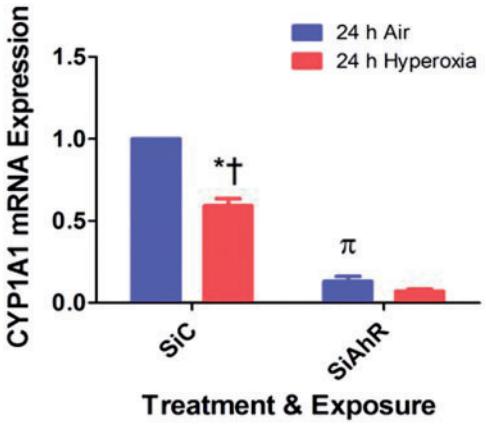

FIG. 10. Real-time RT-PCR analysis of CYP1A1 mRNA expression. Control (SiC) or AhR (SiAhR) siRNA-transfected HPMEC were exposed to normoxia (air) or hyperoxia for up to 24 h, following which RNA was extracted for real-time RT-PCR analyses of CYP1A1 mRNA expression. Data are representative of at least 3 independent experiments. Values are presented as means ± SEM (n = 3). Two-way ANOVA showed an effect of hyperoxia and AhR gene and an interaction between them for the dependent variable, CYP1A1, in this figure. Significant differences between air- and hyperoxia-exposed cells are indicated by *, $P < 0.05$. Significant differences between hyperoxia-exposed AhR-sufficient and -deficient cells are indicated by †, $P < 0.05$. Significant differences between air-exposed cells are indicated by π, $P < 0.05$.

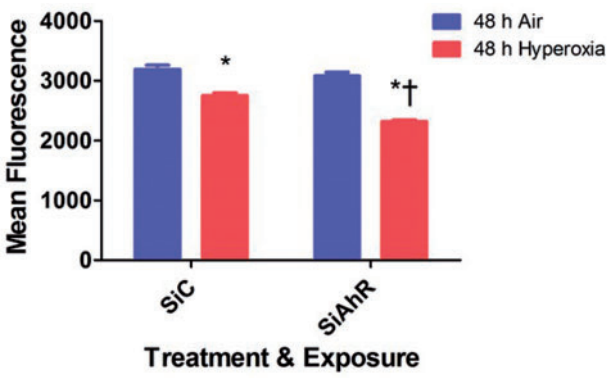

FIG. 11. AhR deficiency potentiates hyperoxia-induced inhibition of cell proliferation. Control (SiC) or AhR (SiAhR) siRNA-transfected HPMEC were exposed to normoxia (air) or hyperoxia for up to 48 h, following which cell proliferation was determined based on the measurement of cellular DNA content via fluorescent dye binding using the CyQUANT NF cell proliferation assay. Values are presented as means ± SEM (n = 3). Data are representative of at least 3 independent experiments. Two-way ANOVA showed an effect of hyperoxia and AhR gene and an interaction between them for cell proliferation. Significant differences between air- and hyperoxia-exposed cells are indicated by *, $P < .05$. Significant differences between hyperoxia-exposed AhR-sufficient and -deficient cells are indicated by †, $P < .05$.

in vivo studies to prevent and/or treat hyperoxia-mediated lung disorders such as BPD in human preterm infants and acute respiratory distress syndrome (ARDS) in older children and adults.

The AhR has been identified as a key regulator of neonatal hyperoxic lung injury both in newborn mice (Bhattacharya *et al.*, 2014; Shivanna *et al.*, 2013) and primary human fetal lung cells (Zhang *et al.*, 2015). To further our understanding of AhR in human neonatal lung biology, we used primary fetal HPMEC since *in vitro* models using human lung cells have been widely used to study the mechanisms of hyperoxic lung injury (Baker *et al.*, 2013; Brahmajothi *et al.*, 2014). Although genome wide transcriptional studies in newborn rodents (Bhattacharya *et al.*, 2014; Chen *et al.*, 2015) have identified several gene expression signatures and pathways including AhR that may be involved in hyperoxic lung injury, there is a need for similar studies in primary fetal human lung cells since it may directly reflect the deregulated genes and pathways in human neonates subjected to hyperoxia. Importantly, lung vascular development and endothelial cell signaling is necessary for alveolarization and disrupted endothelial cell proliferation and signaling can arrest alveolarization, which is the histologic hallmark of modern BPD (Abman, 2001). Hence, we performed a genome wide transcriptional study in HPMEC to identify the deregulated genes and pathways by hyperoxia in general and by the AhR in particular to better understand the molecular mechanisms by which AhR modulates neonatal hyperoxic lung injury. Although, microarray analyses at a single time point could have potentially failed to identify all the deregulated genes and pathways, we identified several novel genes and biological process that were affected in this model.

The majority of the DEGs in AhR-deficient cells were identified in hyperoxic conditions (Figs. 3B and C), indicating that AhR signaling plays an important role in neonatal hyperoxic lung injury. In addition, the finding of 170 deregulated genes (Figs. 3B and C) in AhR-deficient HPMEC exposed to both air and hyperoxic conditions suggest that AhR also induces a general gene expression response -upon exposures to different oxygen concentrations. The major deregulated pathways in AhR-depleted cells (Figure 4) suggest that AhR regulates organ development, cell proliferation, and inflammation. These findings have important implications for the management of BPD, which is a developmental lung disease of premature infants that is characterized by increased inflammation and an interruption in alveolar development. Although AhR has been shown to regulate pathways involved in cell proliferation, apoptosis, inflammation, and liver development in mice (Bunger *et al.*, 2008; Harper *et al.*, 2013; Marlowe *et al.*, 2004; Moura-Alves *et al.*, 2014), our study, which entailed the use of primary human fetal lung cells indicates that AhR may play a role in inflammation, cell proliferation and development of human lungs. Moreover, our study has identified some new AhR-regulated genes such as activin A receptor 2 like 1 (ACVRL1), COL18A1, FABP5, COL4A2, LAMC2, and ETS1 that may contribute to the development of lungs and thereby can be useful biomarkers and potential therapeutic target for disorders of lung development such as BPD.

A number of genes involved in cell proliferation were modulated by hyperoxia in both AhR-sufficient and deficient cells, including KPNA2, ACVRL1, PGF, and CDC20. KPNA2 is an adapter protein that imports signaling factors into the nucleus and exports response molecules into the cytoplasm (Poon and Jans, 2005) and it promotes cell proliferation by facilitating G1/S cell cycle transition (Huang *et al.*, 2013). ACVRL1 is an important member of the TGFβ1/SMAD1/5 signaling pathway in the endothelium (Goumans *et al.*, 2002) and plays a pivotal role in early blood vessel development and remodeling (Oh *et al.*, 2000), which is critical for lung morphogenesis. PGF is a member of vascular endothelial growth factor (VEGF) subfamily and is expressed in placenta, type II alveolar cells and lung endothelial cells (Sands *et al.*, 2011). PGF promotes endothelial proliferation and contributes to angiogenesis by augmenting VEGF signaling (Cao *et al.*, 1996). Cell division cycle 20 (CDC20) is a cell cycle regulatory protein that interacts with several other proteins to promote cell proliferation by activating the anaphase promoting complex, which in turn facilitates the cell to enter anaphase and exit from mitosis (Fang *et al.*, 1998). Our results indicate that

AhR regulates the expression of novel genes such as KPNA2 (Figure 8A), ACVRL1 (Tables 1 and 3), and PGF (Figure 8D). Interventions targeting KPNA2, ACVRL1, and PGF can facilitate alveolar epithelial and endothelial cell proliferation and thereby mitigate the interruption in alveolarization and vascularization in preterm infants at risk for or those who have BPD.

Consistent with the notion that inflammation plays a key role in the pathogenesis of hyperoxia-induced lung disorders such as BPD in preterm infants, and ARDS in older children and adults (Barazzone and White, 2000; Saugstad, 2003), hyperoxia deregulated the expression of inflammatory chemokines (C-C motif) and their ligands (C-X-C L) such as CCL3 (macrophage inflammatory protein 1), CCL5 (regulated on activation, normal T-cell expressed and secreted), and CXCL10 (interferon gamma-induced protein 10) in our experimental model in AhR-deficient cells (Figure 9). These chemokines can recruit and activate granulocytes, monocyte/macrophages, and T cells and initiate an inflammatory response and inhibit angiogenesis thereby contributing to the development of BPD. Several other investigators have suggested these chemokines may be an important mediator of hyperoxia-induced lung injury (Harijith *et al.*, 2011; Nagato *et al.*, 2015; Quintero *et al.*, 2010). Thus, our results in human cells signify the beneficial antiinflammatory role of the AhR in hyperoxia-induced lung disorders in humans.

In alignment with other studies, hyperoxia predominantly deregulated genes that affected cell cycle, cell death, inflammation, and stress response (Bhattacharya *et al.*, 2014; Chambellan *et al.*, 2006; McGrath-Morrow *et al.*, 2014; Perkowski *et al.*, 2003). One of the most interesting findings of our study was that AhR positively regulates the pathways that are necessary for organ morphogenesis, system development, and anatomic organ development (Figure 4). Among the down-regulated pathways in AhR-deficient cells, it is interesting to note that the genes promoting cell cycle arrest and cell proliferation were both down-regulated in air and hyperoxic conditions (Figs. 4 and 6). However, AhR deficiency augmented hyperoxia-mediated inhibition of HPMEC proliferation (Figure 11), which indicates that AhR is a positive regulator of cell proliferation in our experimental conditions. This was in contrast to other studies where AhR activation is shown to inhibit cell proliferation (Jackson *et al.*, 2014; Li *et al.*, 2015). Some of the contributing factors might be related to the nature of ligands (exogenous vs endogenous), cell or tissue specificity, developmental stage of the tissue/animal, and the nature of experimental insult.

Real-time RT-PCR was used to verify the microarray data for 6 DEG and there was a good correlation between the RT-PCR and microarray data. The gene expression was underestimated for the chemokines, CCL5, and CXCL10, on the microarrays, which may have resulted in few false negative data. The disparities in the fold change between microarray and RT-PCR analysis may be related to their differences in the sensitivities and mechanisms of detection of gene expression. However, the data obtained from both the techniques were qualitatively similar. Interestingly, the classical AhR-regulated CYP1A1 gene was not repressed on microarrays, but was found to be significantly repressed by real time RT-PCR in AhR-deficient cells (Figure 10). A similar finding has been observed by other investigators who have attributed this to very low constitutive expression of CYP1A genes in the cells (Staal *et al.*, 2006).

In summary, this study characterizes the gene expression profile of AhR-deficient cells in air and hyperoxic conditions and thereby provides an insight into the cellular response to AhR deficiency, oxygen exposure, and the combination of the 2. Our study not only confirms known AhR- and hyperoxia-regulated genes and pathways, but also sheds light on novel genes and pathways deregulated by AhR, hyperoxia, and a combination of the 2. By performing a functional analysis such as cell proliferation assay, we have further elucidated a major molecular mechanism by which AhR regulates hyperoxic lung injury. Our findings further emphasizes that AhR regulates hyperoxic lung injury and thereby is a potential therapeutic target in the management of hyperoxia-induced disorders such as BPD in preterm infants and ARDS in older children and adults.

ACKNOWLEDGEMENTS

We thank the Laboratory for Translational Genomics at Baylor College of Medicine led by John Belmont for performing the microarray experiments and analysis.

FUNDING

This work was supported by grants from National Institutes of Health (K08 HD073323 to B.S. and R01 ES009132, R01 HL112516, R01 HL087174, and R01 ES019689 to B.M.); American Heart Association (BGIA 20190008 to B.S); and Alkek Foundation (Molecular Discovery Pilot grant to C.C.). The study sponsors had no involvement in study design, data collection, analysis and interpretation, writing of the report or decision to submit the article for publication.

REFERENCES

Abman, S. H. (2001). Bronchopulmonary dysplasia: "a vascular hypothesis". *Am. J. Respir. Crit. Care Med.* **164**, 1755–1756.

Ashburner, M., Ball, C. A., Blake, J. A., Botstein, D., Butler, H., Cherry, J. M., Davis, A. P., Dolinski, K., Dwight, S. S., Eppig, J. T., *et al.* (2000). Gene ontology: tool for the unification of biology. The Gene Ontology Consortium. *Nat. Genet.* **25**, 25–29.

Baglole, C. J., Maggirwar, S. B., Gasiewicz, T. A., Thatcher, T. H., Phipps, R. P., and Sime, P. J. (2008). The aryl hydrocarbon receptor attenuates tobacco smoke-induced cyclooxygenase-2 and prostaglandin production in lung fibroblasts through regulation of the NF-kappaB family member RelB. *J. Biol. Chem.* **283**, 28944–28957.

Baker, C. D., Seedorf, G. J., Wisniewski, B. L., Black, C. P., Ryan, S. L., Balasubramaniam, V., and Abman, S. H. (2013). Endothelial colony-forming cell conditioned media promote angiogenesis in vitro and prevent pulmonary hypertension in experimental bronchopulmonary dysplasia. *American J. Physiol. Lung Cell. Mol. Physiol.* **305**, L73–L81.

Barazzone, C., and White, C. W. (2000). Mechanisms of cell injury and death in hyperoxia: role of cytokines and Bcl-2 family proteins. *Am. J. Respir. Cell Mol. Biol.* **22**, 517–519.

Bhattacharya, S., Zhou, Z., Yee, M., Chu, C. Y., Lopez, A. M., Lunger, V. A., Solleti, S. K., Resseguie, E., Buczynski, B., Mariani, T. J., and., *et al.* (2014). The genome-wide transcriptional response to neonatal hyperoxia identifies Ahr as a key regulator. *Am. J. Physiol.. Lung Cell. Mol. Physiol.* **307**, L516–L523.

Bock, K. W., and Kohle, C. (2009). The mammalian aryl hydrocarbon (Ah) receptor: from mediator of dioxin toxicity toward physiological functions in skin and liver. *Biol. Chem.* **390**, 1225–1235.

Brahmajothi, M. V., Tinch, B. T., Wempe, M. F., Endou, H., and Auten, R. L. (2014). Hyperoxia inhibits nitric oxide treatment

effects in alveolar epithelial cells via effects on L-type amino acid transporter-1. *Antioxid. Redox. Signal.* **21**, 1823–1836.

Bunger, M. K., Glover, E., Moran, S. M., Walisser, J. A., Lahvis, G. P., Hsu, E. L., and Bradfield, C. A. (2008). Abnormal liver development and resistance to 2,3,7,8-tetrachlorodibenzo-p-dioxin toxicity in mice carrying a mutation in the DNA-binding domain of the aryl hydrocarbon receptor. *Toxicol. Sci.* **106**, 83–92.

Burbach, K. M., Poland, A., and Bradfield, C. A. (1992). Cloning of the Ah-receptor cDNA reveals a distinctive ligand-activated transcription factor. *Proc. Natl. Acad. Sci. U S A* **89**, 8185–8189.

Cao, Y., Linden, P., Shima, D., Browne, F., and Folkman, J. (1996). In vivo angiogenic activity and hypoxia induction of heterodimers of placenta growth factor/vascular endothelial growth factor. *J. Clin. Invest.* **98**, 2507–2511.

Chambellan, A., Cruickshank, P. J., McKenzie, P., Cannady, S. B., Szabo, K., Comhair, S. A., and Erzurum, S. C. (2006). Gene expression profile of human airway epithelium induced by hyperoxia in vivo. *Am. J. Respir. Cell Mol. Biol.* **35**, 424–435.

Chen, X., Walther, F. J., Sengers, R. M., Laghmani el, H., Salam, A., Folkerts, G., Pera, T., and Wagenaar, G. T. (2015). Metformin attenuates hyperoxia-induced lung injury in neonatal rats by reducing the inflammatory response. *Am. J Physiol. Lung Cell. Mol. Physiol.* **309**, L262–L270.

Couroucli, X. I., Welty, S. E., Geske, R. S., and Moorthy, B. (2002). Regulation of pulmonary and hepatic cytochrome P4501A expression in the rat by hyperoxia: implications for hyperoxic lung injury. *Mol. Pharmacol.* **61**, 507–515.

Croft, D., Mundo, A. F., Haw, R., Milacic, M., Weiser, J., Wu, G., Caudy, M., Garapati, P., Gillespie, M., Kamdar, M. R., *et al.* (2014). The Reactome pathway knowledgebase. *Nucleic Acids Res.* **42**, D472–D477.

Du, P., Kibbe, W. A., and Lin, S. M. (2008). lumi: a pipeline for processing Illumina microarray. *Bioinformatics* **24**, 1547–1548.

Emi, Y., Ikushiro, S., and Iyanagi, T. (1996). Xenobiotic responsive element-mediated transcriptional activation in the UDP-glucuronosyltransferase family 1 gene complex. *J. Biol. Chem.* **271**, 3952–3958.

Fanaroff, A. A., Stoll, B. J., Wright, L. L., Carlo, W. A., Ehrenkranz, R. A., Stark, A. R., Bauer, C. R., Donovan, E. F., Korones, S. B., Laptook, A. R., *et al.* (2007). Trends in neonatal morbidity and mortality for very low birthweight infants. *Am. J. Obstet. Gynecol.* **196**, 147 e141–148.

Fang, G., Yu, H., and Kirschner, M. W. (1998). The checkpoint protein MAD2 and the mitotic regulator CDC20 form a ternary complex with the anaphase-promoting complex to control anaphase initiation. *Genes Dev.* **12**, 1871–1883.

Favreau, L. V., and Pickett, C. B. (1991). Transcriptional regulation of the rat NAD(P)H:quinone reductase gene. Identification of regulatory elements controlling basal level expression and inducible expression by planar aromatic compounds and phenolic antioxidants. *J. Biol. Chem.* **266**, 4556–4561.

Fujii-Kuriyama, Y., and Kawajiri, K. (2010). Molecular mechanisms of the physiological functions of the aryl hydrocarbon (dioxin) receptor, a multifunctional regulator that senses and responds to environmental stimuli. *Proc. Jpn Acad. Ser. B Phys. Biol. Sci.* **86**, 40–53.

Goumans, M. J., Valdimarsdottir, G., Itoh, S., Rosendahl, A., Sideras, P., and ten Dijke, P. (2002). Balancing the activation state of the endothelium via two distinct TGF-beta type I receptors. *EMBO J.* **21**, 1743–1753.

Harijith, A., Choo-Wing, R., Cataltepe, S., Yasumatsu, R., Aghai, Z. H., Janer, J., Andersson, S., Homer, R. J., and Bhandari, V. (2011). A role for matrix metalloproteinase 9 in IFNgamma-mediated injury in developing lungs: relevance to bronchopulmonary dysplasia. *Am. J. Respir. Cell Mol. Biol.* **44**, 621–630.

Harper, T. A., Jr., Joshi, A. D., and Elferink, C. J. (2013). Identification of stanniocalcin 2 as a novel aryl hydrocarbon receptor target gene. *J. Pharmacol. Exp. Ther.* **344**, 579–588.

Huang, L., Wang, H. Y., Li, J. D., Wang, J. H., Zhou, Y., Luo, R. Z., Yun, J. P., Zhang, Y., Jia, W. H., and Zheng, M. (2013). KPNA2 promotes cell proliferation and tumorigenicity in epithelial ovarian carcinoma through upregulation of c-Myc and downregulation of FOXO3a. *Cell Death Dis.* **4**, e745.

Husain, A. N., Siddiqui, N. H., and Stocker, J. T. (1998). Pathology of arrested acinar development in postsurfactant bronchopulmonary dysplasia. *Hum. Pathol.* **29**, 710–717.

Jackson, D. P., Li, H., Mitchell, K. A., Joshi, A. D., and Elferink, C. J. (2014). Ah receptor-mediated suppression of liver regeneration through NC-XRE-driven p21Cip1 expression. *Mol. Pharmacol.* **85**, 533–541.

Jiang, W., Welty, S. E., Couroucli, X. I., Barrios, R., Kondraganti, S. R., Muthiah, K., Yu, L., Avery, S. E., and Moorthy, B. (2004). Disruption of the Ah receptor gene alters the susceptibility of mice to oxygen-mediated regulation of pulmonary and hepatic cytochromes P4501A expression and exacerbates hyperoxic lung injury. *J. Pharmacol. Exp. Ther.* **310**, 512–519.

Jobe, A. H., Hillman, N., Polglase, G., Kramer, B. W., Kallapur, S., and Pillow, J. (2008). Injury and inflammation from resuscitation of the preterm infant. *Neonatology* **94**, 190–196.

Kanehisa, M., Goto, S., Sato, Y., Kawashima, M., Furumichi, M., and Tanabe, M. (2014). Data, information, knowledge and principle: back to metabolism in KEGG. *Nucleic Acids Res.* **42**, D199–D205.

Kato, H., Shichiri, M., Marumo, F., and Hirata, Y. (1997). Adrenomedullin as an autocrine/paracrine apoptosis survival factor for rat endothelial cells. *Endocrinology* **138**, 2615–2620.

Li, Y., Wang, K., Zou, Q. Y., Magness, R. R., and Zheng, J. (2015). 2,3,7,8-Tetrachlorodibenzo-p-dioxin differentially suppresses angiogenic responses in human placental vein and artery endothelial cells. *Toxicology* **336**, 70–78.

Lindsey, S., and Papoutsakis, E. T. (2012). The evolving role of the aryl hydrocarbon receptor (AHR) in the normophysiology of hematopoiesis. *Stem Cell Rev.* **8**, 1223–1235.

Marlowe, J. L., Knudsen, E. S., Schwemberger, S., and Puga, A. (2004). The aryl hydrocarbon receptor displaces p300 from E2F-dependent promoters and represses S phase-specific gene expression. *J. Biol. Chem.* **279**, 29013–29022.

McGrath-Morrow, S. A., Lauer, T., Collaco, J. M., Lopez, A., Malhotra, D., Alekseyev, Y. O., Neptune, E., Wise, R., and Biswal, S. (2014). Transcriptional responses of neonatal mouse lung to hyperoxia by Nrf2 status. *Cytokine* **65**, 4–9.

Moura-Alves, P., Fae, K., Houthuys, E., Dorhoi, A., Kreuchwig, A., Furkert, J., Barison, N., Diehl, A., Munder, A., Constant, P., *et al.* (2014). AhR sensing of bacterial pigments regulates antibacterial defence. *Nature* **512**, 387–392.

Nagato, A. C., Bezerra, F. S., Talvani, A., Aarestrup, B. J., and Aarestrup, F. M. (2015). Hyperoxia promotes polarization of the immune response in ovalbumin-induced airway inflammation, leading to a TH17 cell phenotype. *Immun. Inflamm. Dis.* **3**, 321–337.

Oh, S. P., Seki, T., Goss, K. A., Imamura, T., Yi, Y., Donahoe, P. K., Li, L., Miyazono, K., ten Dijke, P., Kim, S., and., *et al.* (2000). Activin receptor-like kinase 1 modulates transforming growth factor-beta 1 signaling in the regulation of angiogenesis. *Proc. Natl. Acad. Sci. U S A* **97**, 2626–2631.

Perkowski, S., Sun, J., Singhal, S., Santiago, J., Leikauf, G. D., and Albelda, S. M. (2003). Gene expression profiling of the early pulmonary response to hyperoxia in mice. *Am. J. Respir. Cell Mol. Biol.* **28**, 682–696.

Poon, I. K., and Jans, D. A. (2005). Regulation of nuclear transport: central role in development and transformation? *Traffic* **6**, 173–186.

Quintero, P. A., Knolle, M. D., Cala, L. F., Zhuang, Y., and Owen, C. A. (2010). Matrix metalloproteinase-8 inactivates macrophage inflammatory protein-1 alpha to reduce acute lung inflammation and injury in mice. *J. Immunol.* **184**, 1575–1588.

Rushmore, T. H., King, R. G., Paulson, K. E., and Pickett, C. B. (1990). Regulation of glutathione S-transferase Ya subunit gene expression: identification of a unique xenobiotic-responsive element controlling inducible expression by planar aromatic compounds. *Proc. Natl. Acad. Sci. U S A* **87**, 3826–3830.

Sands, M., Howell, K., Costello, C. M., and McLoughlin, P. (2011). Placenta growth factor and vascular endothelial growth factor B expression in the hypoxic lung. *Respir. Res.* **12**, 17.

Saugstad, O. D. (2003). Bronchopulmonary dysplasia-oxidative stress and antioxidants. *Semin. Neonatol.* **8**, 39–49.

Saugstad, O. D. (2010). Oxygen and oxidative stress in bronchopulmonary dysplasia. *J. Perinat. Med.* **38**, 571–577.

Sauzeau, V., Carvajal-Gonzalez, J. M., Riolobos, A. S., Sevilla, M. A., Menacho-Marquez, M., Roman, A. C., Abad, A., Montero, M. J., Fernandez-Salguero, P., and Bustelo, X. R. (2011). Transcriptional factor aryl hydrocarbon receptor (Ahr) controls cardiovascular and respiratory functions by regulating the expression of the Vav3 proto-oncogene. *J. Biol. Chem.* **286**, 2896–2909.

Shivanna, B., Chu, C., Welty, S. E., Jiang, W., Wang, L., Couroucli, X. I., and Moorthy, B. (2011). Omeprazole attenuates hyperoxic injury in H441 cells via the aryl hydrocarbon receptor. *Free Radic. Biol. Med.* **51**, 1910–1917.

Shivanna, B., Zhang, W., Jiang, W., Welty, S. E., Couroucli, X. I., Wang, L., and Moorthy, B. (2013). Functional deficiency of aryl hydrocarbon receptor augments oxygen toxicity-induced alveolar simplification in newborn mice. *Toxicol. Appl. Pharmacol.* **267**, 209–217.

Short, E. J., Klein, N. K., Lewis, B. A., Fulton, S., Eisengart, S., Kercsmar, C., Baley, J., and Singer, L. T. (2003). Cognitive and academic consequences of bronchopulmonary dysplasia and very low birth weight: 8-year-old outcomes. *Pediatrics* **112**, e359.

Staal, Y. C., van Herwijnen, M. H., van Schooten, F. J., and van Delft, J. H. (2006). Modulation of gene expression and DNA adduct formation in HepG2 cells by polycyclic aromatic hydrocarbons with different carcinogenic potencies. *Carcinogenesis* **27**, 646–655.

Subramanian, A., Tamayo, P., Mootha, V. K., Mukherjee, S., Ebert, B. L., Gillette, M. A., Paulovich, A., Pomeroy, S. L., Golub, T. R., Lander, E. S., and., *et al.* (2005). Gene set enrichment analysis: a knowledge-based approach for interpreting genome-wide expression profiles. *Proc. Natl. Acad. Sci. U S A* **102**, 15545–15550.

Thatcher, T. H., Maggirwar, S. B., Baglole, C. J., Lakatos, H. F., Gasiewicz, T. A., Phipps, R. P., and Sime, P. J. (2007). Aryl hydrocarbon receptor-deficient mice develop heightened inflammatory responses to cigarette smoke and endotoxin associated with rapid loss of the nuclear factor-kappaB component RelB. *Am. J. Pathol.* **170**, 855–864.

Thiel, M., Chouker, A., Ohta, A., Jackson, E., Caldwell, C., Smith, P., Lukashev, D., Bittmann, I., and Sitkovsky, M. V. (2005). Oxygenation inhibits the physiological tissue-protecting mechanism and thereby exacerbates acute inflammatory lung injury. *PLoS Biol.* **3**, e174.

Wettenhall, J. M., and Smyth, G. K. (2004). limmaGUI: a graphical user interface for linear modeling of microarray data. *Bioinformatics* **20**, 3705–3706.

Wright, C. J., Agboke, F., Chen, F., La, P., Yang, G., and Dennery, P. A. (2010). NO inhibits hyperoxia-induced NF-kappaB activation in neonatal pulmonary microvascular endothelial cells. *Pediatr. Res.* **68**, 484–489.

Wright, C. J., and Kirpalani, H. (2011). Targeting inflammation to prevent bronchopulmonary dysplasia: can new insights be translated into therapies? *Pediatrics* **128**, 111–126.

Zhang, S., Patel, A., Chu, C., Jiang, W., Wang, L., Welty, S. E., Moorthy, B., and Shivanna, B. (2015). Aryl hydrocarbon receptor is necessary to protect fetal human pulmonary microvascular endothelial cells against hyperoxic injury: Mechanistic roles of antioxidant enzymes and RelB. *Toxicol. Appl. Pharmacol.* **286**, 92–101.